

Could *Acinetobacter baumannii* Lol-abaucin docking be improved?

short title: anti-LolCE *A.baumannii* antibiotics

Coll, J*.

Department of Biotechnology. Centro Nacional INIA-CSIC. Madrid, Spain.

* Corresponding author

Emails: julio.coll.m@csic.es; juliocollm@gmail.com

Julio Coll, orcid: 0000-0001-8496-3493

Abstract

To explore alternative abaucin antibiotics predicting nanomolar affinities against *Acinetobacter baumannii*, thousands of virtual abaucin-derived molecules were randomly generated and selected. For this, alphafold-modeled *A.baumannii* lipoprotein outer membrane localization (Lol) complex proteins were targeted by DataWarrior "build evolutionary libraries". Abaucin-children libraries were generated from the abaucin-parent iteratively selecting those predicting higher affinities to the most probable *A.baumannii* LolCE docking-cavity. To improve accuracies, ~4000 abaucin-children docking-scores were consensed with those from AutoDockVina. The resulting laydown table provided with filter sliders would allow user-criteria to be applied. One example explored candidates predicting both higher nanomolar affinities to *A.baumannii* LolCE (to favor putative antibiotics) and lower affinities to *E.coli* LolCE (to favor narrow-bacterial spectrum hits). Despite being highly hypothetical, some of these abaucin-derived chemotypes may constitute another step towards exploring possible improvements for anti-*A.baumannii* antibiotics.

Keywords: LolCE; lipoprotein transporter; *Acinetobacter baumannii*; evolutionary libraries; docking; antibiotics

Introduction

Most recently, a deep-learning guided study predicted a novel antibiotic against *Acinetobacter baumannii*, which was named abaucin¹. Chemically synthesized abaucin and derivatives inhibited *in vitro* *A.baumannii* growth at the low micromolar range (~5 μM) and suppressed *A.baumannii* in a wound-infected mice model. Furthermore, abaucin displayed a desirable narrow bacterial spectrum which would favor host microbiota preservation during treatment, in contrast to many other antibiotics. In particular, abaucin was discovered by training a deep-learning model with a chemical library of 7500 molecules obtained from patented and synthetic origins. Briefly, 6.2% inhibited *A.baumannii* *in vitro* growth at < 50 μM (active molecules). A training-set containing active and inactive virtual molecules computationally trained a deep-learning model. Finally, screening of the Drug Repurposing Hub library² with the deep-learning model, predicted high affinity compounds and discovered the abaucin lead¹. Additional molecular mechanistic studies found out that abaucin perturbs lipoprotein trafficking in *A. baumannii* by interacting with the lipoprotein outer membrane localization (Lol) protein complex.

A. baumannii is a Gram-negative bacteria causing health care-associated infections resistant to multiple antibiotics³⁻⁵. For instance, *A. baumannii* is a leading cause of nosocomial infections, particularly in intensive care units. It can cause pneumonia, bloodstream, urinary tract, and surgical site infections associated with high mortality rates. The ability of *A. baumannii* for environmental persistence and for dissemination of antibiotic-resistance genes is a global concern⁶. *A. baumannii* has demonstrated resistance to a wide range of antimicrobial agents, including carbapenems, which are considered the last line of defense against multidrug-resistant bacteria⁷. The increasing emergence of pan-drug resistant *A. baumannii* strains further limits treatment options constituting an emerging target aspect for new drug discovery^{8,9}. Identification of novel antibiotics against *A. baumannii* is crucial for world wide healthcare^{10,11}.

The abaucin-targeted Lol protein complexes are among the under explored bacterial targets that may be an appropriated source for new anti-bacterial treatments. In Gram negative bacteria such as *A. baumannii* or *E.coli*, Lol proteins transport signaled lipoproteins from their internal to their external outer compact membranes. External outer bacterial membrane lipoproteins cause most of their resistance to penetration of antibiotics. Mislocalization of the Lol protein complexes results in bacterial death. Small-molecule inhibitors of lipoprotein transport have shown antibacterial activities. However, most of present Lol-targeted antibiotics, including abaucin are active against *A. baumannii* at low micromolar ranges^{7,12-17}. There may be room for affinity improvements.

Lol complexes involve 3-5 different proteins depending on the lipoprotein transport stages¹⁸. *E.coli* LolCDE consists of a CE protein heterodimer inserted in the bacterial membranes through C4+E4 transmembrane α-helices and projecting outside their head and cytosolic domains. With a sequence identity of only 14.6%, C and E proteins form dimerization interfaces with C2+E2 α-helical V shaped central lipoprotein-binding cavity extending above ~20 Å out the bacterial membranes. The LolCE complex is maintained together by a DD homodimer interacting with the cytosolic domains down the membrane. Purified *E.coli* LolCDE revealed a number of lipoprotein ligands. Most ligands contain one 9-10 amino acid peptide upwards linked to three downward hydrophobic triacyl chains. The other LolC2+E2 α-helices, sterically prevent any possible scape of the bound

lipoproteins (Figure 1). The DD dimer shows ATP-binding capacities implicating ATP hydrolysis in LolCE open/close conformational changes. Protein A binds above C and also participate in the conformational changes (RMSD 3.6-4.8 Å). Conformational changes facilitate ATP hydrolysis, inner to outer membrane transport and delivery of the lipoprotein¹⁸.

E.coli mutants in the upper part of their E protein such as LolCDE(D264A), Lol CDE(I268D), LolCDE(Y366A) and LolCDE(F367D) reduced lipoprotein binding and were lethal¹⁸. In contrast, other mutants surrounding the lipoprotein triacyl chains in the protein C like LolC(M48G)DE, LolC(M267E)DE or LolC(L356D)DE, were not lethal. Mutants in the D proteins caused disintegration of the LolCDE complex. The results of all these studies, suggest that the peptide moieties of lipoproteins mostly interact with the E protein at the LolCDE complexes and that the lipoprotein peptide-binding residues at the upper part of E, may be essential for LolCDE transport. The mutational studies and the crystal structures briefly commented above, clarified *E.coli* lipoprotein transport mechanisms and allowed an hypothetical probable modeling of the *A. baumannii* LolCE. Accordingly, the upper α-helices of the E protein modeled in the *A. baumannii* LolCE heterodimer have been targeted here to study abaucin-derivatives.

Abaucin was selected as parent to generate children molecules because it is among the most recently described antibiotics anti-*A.baumannii* displaying low micromolar activities. The LolCE model was selected as target because despite the absence of a crystallographic abaucin-bound *A.baumannii* model, the elucidated *E.coli* LolCDE protein complex 3D structure¹⁶ could be used to predict an alphafold *A.baumannii* model with high accuracy (Figure 1).

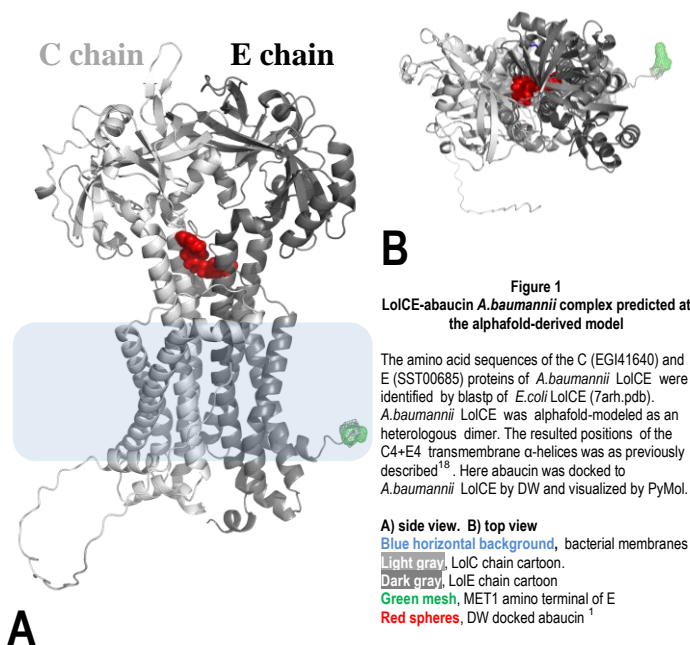
To explore a possible expansion of abaucin-derived chemotypes predicting nanomolar activities, we choose the "build evolutionary library" generation algorithm described at the DataWarrior (DW) program. This algorithm has been similarly applied on our predictions targeting other protein-ligand pair examples¹⁹⁻²¹. This generation/selection algorithm offers a unique alternative to the screening of large chemical data banks or to the deep-learning discovery methods. The here called evolutionary docking library augmented the repertoire of abaucin-derived children by generating ~45000 new molecules by small chemical random changes. Only those children predicting improved affinity to the abaucin *A. baumannii* LolCE docking-cavity were selected for iterative generations. Thousands of abaucin-children with improved fitting to the abaucin docking-cavity could be generated by this method. Additionally, since *E.coli* is the most important commensal specie, DW docking to the crystallographic *E.coli* LolCDE target was employed to eliminate those *A. baumannii* abaucin-children with *E.coli* undesirable high affinities. The abaucin-children candidates predicting DW high affinities (low docking-scores) to *A. baumannii* LolCDE by both DW and AutoDockVina (ADV) were consensed to increase the accuracy of their predictions. While these results are uncertain due to be based only on a computationally predicted model and ligand putative candidates, the proposed list displayed numerous alternatives with higher affinities than abaucin.

The most recent successful inhibitory activity of the computationally guided abaucin¹, the availability of crystallized *E.coli* LolCDE models¹⁸, the accuracy improvements in modeling proteins by alphafold²², and the application of recent DW build evolutionary library predictive algorithms¹⁹⁻²¹, have been combined here to computationally extend hypothetical new abaucin-derived chemotypes predicting nanomolar affinities for future antibiotic candidates against *A. baumannii*.

Computational Methods

LoICE *A.baumannii* alphafold modeling

The 7arh.pdb crystallographic model of *E.coli* lipoprotein outer membrane localization (Lol) was retrieved from the RCSB bank (<https://www.rcsb.org/>)¹⁸. The amino acid sequences of blastp C (EG141640) and E (SST00685) chains of *A.baumannii* LoICE were identified from the corresponding *E.coli* protein C and E sequences at 7arh.pdb (<http://www.ncbi.nlm.nih.gov/sites/entrez?db=nucleotide>). The C and E *A.baumannii* protein sequences were then modeled as one heterologous dimer with the Sokrypton AlphaFold2.ipynb Colab (<https://colab.research.google.com/github/sokrypton/ColabFold/blob/main/AlphaFold2.ipynb>)²². The *A.baumannii* LoICE model predicting the lowest RMSD (Root Square Mean Differences) of 3.6 Å with the *E.coli* 7arh.pdb CE dimer, was selected for further work. The 4+4 CE transmembrane α -helices of the *A.baumannii* alphafold model could be mapped in a similar position than those previously described for *E.coli*¹⁸ (Figure 1AB). Abaucin was docked to *A.baumannii* LoICE by ADV and DW and visualized in PyMol. For DW docking, the pdb files required elimination of the CONNECT lines.



Generation of abaucin-children

The "Build Evolutionary Library" and "Dock Structures into Docking Cavity" subprograms included into DataWarrior (DW)⁴⁶ were used here to generate abaucin-derivative libraries fitting the abaucin docking-cavity (evolutionary docking libraries), following our previous more detailed descriptions¹⁹⁻²¹. Common evolutionary parameters such as generations of 128 children, selection of 16 children per generation, preference for drug-like properties and 3 runs were chosen as optimized in previous work. Children from the abaucin parent, were first predicted by fitting to higher affinity to the ADV and DW identified abaucin-docking cavities (evolutionary docking). Molecular weight restriction criteria were then added to the fitting criteria but maintaining the highest relative weight for affinity (x4). Additional molecular weight (2x) and logP (x1) fitting criteria were added to subsequent evolutionary docking. As indicated before, the abaucin-children were saved as *.dwar files and filtered by excluding any toxic DW chemical properties (mutagenesis, tumorigenicity, reproductive interference, irritant, and nasty functions) using a home-designed `toxicprediction.dwam` macro (included in the Supplementary Material). Non-toxic children were saved as *.dwar and special *.sdf (vs3) files^{19, 20}

Computational programs

The "Build evolutionary library" and "Dock Structures into Docking Cavity" subprograms included into the DataWarrior (DW)⁴⁶ (dw550win.zip for Windows) were obtained (<https://openmolecules.org/datawarrior/download.html>) as described at DW and our previous work¹⁹⁻²¹. The AutoDockVina (ADV) program written in Python vs3.8 and included in the PyRx-098/PyRx-1.0 package was used as described before (<https://pyrx.sourceforge.io/>)¹⁹. The MolSoft program (ICM Molbrowser vs3.9Win64bit (<https://www.molsoft.com/download.html>)) was used for easier manipulation of the *.sdf files and for drawing 2D molecular structures. The Origin program (OriginPro 2022, 64 bit, Northampton, MA, USA) (<https://www.originlab.com/>) was used for calculations and figure drawings. The

predicted structures were visualized mostly in PyMOL 2.5.3

(<https://www.pymol.org/>) but also in PyRx 098/PyRx1.0 (Mayavi), and Discover Studio Visualizer v21.1.0.20298 (Dassault Systemes Biovia Corp, 2020, <https://discover.3ds.com/discovery-studio-visualizer-download>). Hydrophobic and Hydrogen-bonded amino acid interactions predicted by the docked ligand complexes were identified by LigPlus vs2.2.8 (<https://www.ebi.ac.uk/thornton-srv/software/LigPlus/download.htm>), and internally visualized using PyMol. A multithreading multi-core i9 (47 CPU) PCSpecialist (AMD Ryzen Threadripper 3960X) provided with 64 Gb of RAM (Corsair Vengeance DDR4 at 3200 MHz, 4 x 16 GB) (<https://www.pcspecialist.es/>) was used for computation.

Results

To define one abaucin docking-cavity on *A.baumannii* LoICE, the crystallographic *E.coli* Lol structure template was employed for modeling¹⁸. After alphafold-modeling, a possible abaucin docking cavity in *A.baumannii* LoICE was predicted by ADV docking simulation. Because some molecular alterations were observed in the abaucin geometry after docking (not shown), the resulted ADV-cavity was used for abaucin docking by DW. The new *A.baumannii* LoICE DW docking-cavity was similar to that obtained from ADV docking but with the advantage of preserving 100 % of the abaucin chemical geometry (Figure 1, AB). Both *A.baumannii* LoICE-abaucin ADV and DW docking cavities were applied for the subsequent evolutionary docking.

Children from the abaucin-parent were first generated by maximizing affinities (minimizing docking-scores) as the unique criteria to explore the molecular characteristics of any possible predictions. After eliminating those children predicting known DW toxicities, the highest children affinities were found at mean molecular weights of 476 ± 52 g/mol and mean logP hydrophobicities of 6.1 ± 1.6 (Figure S1).

Molecular weight criteria between 300 to 550 g/mol maintaining logP < 4, were added for additional evolutionary dockings. Using both ADV or DW abaucin-docking cavities, thousands of abaucin-children fitting their corresponding *A.baumannii* LoICE cavities predicted higher affinities (Figure 2, horizontal dashed blue line) than those predicted for the abaucin-parent (~ DW docking-scores < -78). The number of raw-children generated per experiment varied from 33387 to 46067 with different molecular weight targets (Table S1). The percentage of raw children predicting best fitting to the criteria mentioned above were almost constant since only varied from 14.5 to 15.4 %. Fitted children that were non-toxic varied from 15.4 to 69.8 %. The children predicted with non-restricted and < 550 g/mol molecular weights, predicted the highest affinities as shown by analyzing their rank profiles of docking-scores vs docking-score order (Figure 2, red stars and spheres). The children predicted with non-restricted and < 550 g/mol molecular weights, were selected to further studies.

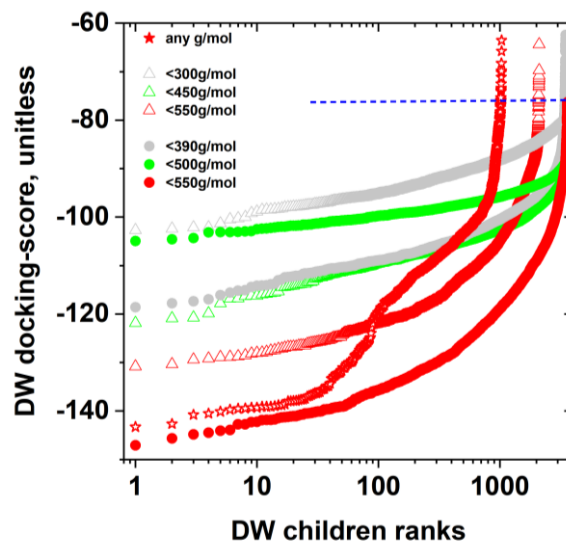


Figure 2
Evolutionary docking rank profiles of abaucin-children at different molecular weights

DW "Build Evolutionary Libraries" using ADV or DW docking cavities at different Molecular Weights (MW, g/mol) generated the abaucin- children described at Table S1. Non-toxic children are represented. The abaucin molecular weight is 390 g/mol.
 Open triangles, abaucin fitted to ADV docking-cavity (abaucin altered geometry)
 Closed spheres, abaucin fitted to DW docking-cavity (abaucin conserved geometry).
 Horizontal dashed blue line, abaucin DW and ADV docking-scores
 Red open stars, any MW (Figure S1)
 Gray triangles, MW <300 g/mol
 Green triangles, MW <450 g/mol
 Red triangles, MW <550 g/mol
 Gray spheres, MW <390 g/mol
 Green spheres, MW <500 g/mol
 Red spheres, MW <550 g/mol

Therefore, the abaucin-children predicted when using no molecular weight restrictions were pooled with those restricted when using <550 g/mol molecular weights. The children predicting > -90 docking-scores (low affinities), <250 g/mol molecular weights (low specificity), and duplicated were removed to obtain an abaucin-children library. The abaucin-children library contained 4312 abaucin-children, predicting between -90 to -145 DW docking-scores, 336 to 550 g/mol molecular weights, and -2.4 to 4.0 logP (4312AbaucinChildrenLibrary.dwar, Supplementary material).

Next, the abaucin-children that predicted high affinities to *E. coli* LolCE (an example of commensal Gram-negative bacteria) were removed. DW docking results predicted very few *E. coli* LolCE abaucin-children with affinities greater or equal to those corresponding to *A. baumannii* and therefore the number of children were maintained (Figure S2). These surprising results suggest that the predicted LolCE abaucin-children are highly specific to *A. baumannii*. They may be innocuous to other commensal bacterial species, if used at appropriated concentrations. Similar computational analysis of any other commensal bacterial species could be performed as their additional Lol structures will become available. Experimental evidences will be required to confirm these hypothesis.

To increase the accuracy of the abaucin-children library predictions, their DW docking-scores were consensed with those obtained by the ADV docking algorithm. ADV was chosen because it relies in a complete different algorithm than DW docking. The DW *A. baumannii* and *E. coli* docking-scores together with ADV *A. baumannii* docking-scores corrected by ligand efficiency (LELP parameter) were displayed together in a unique DW table containing the ~ 4000 abaucin-children library. This DW table allow multiple filter thresholds to be simultaneously user-applied for each of the abaucin-children *A. baumannii* (DWa, DWe, ADVa, LELPa, a=*A. baumannii*, e=*E. coli*), including also their molecular weights and logP properties (4312AbaucinChildrenLibrary.dwar, Supplementary Material).

To show the results of a prove-of-concept example of the above mentioned possibilities for candidate selection, stringent <-100 DW docking-score thresholds were applied to retain only the highest affinities to *A. baumannii* LolCE (lead predicted antibiotics). In contrast, those children predicting also high affinities (<76 DW docking-scores) to *E. coli* LolCE, were skipped (avoid commensal antibiotics). The so downsized abaucin children library was further refined by consensus docking by selecting for those children predicting also *A. baumannii* LolCE ADV scores <100 nM (high affinities) and also by taking into account their minimal calculated ligand efficiency LELP parameters. This example of simultaneous filter combinations, predicted the abaucin-children leads **18544** and **34326** (Table S2 and Figure 3) Other threshold combinations may be chosen to predict other *A. baumannii* LolCE children for particular user purposes (4312AbaucinChildrenLibrary.dwar, Supplementary Material).

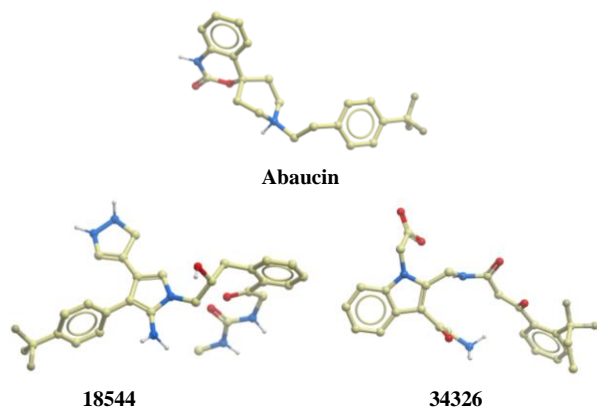


Figure 3
Representative 2D molecule examples of abaucin and their abaucin-children
Red, Oxygens. Blue, Nitrogens

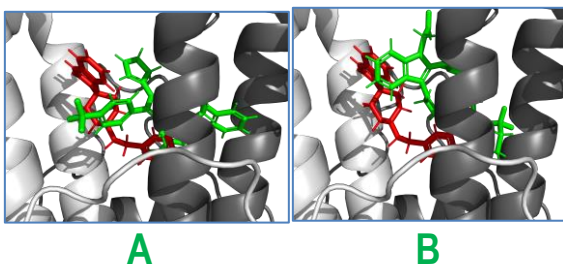


Figure 4
Mapping of representative 18554 (A) and 34326 (B) compared to abaucin (red sticks) DW-docked to *A. baumannii* LolCE
Light gray, protein C. Darker gray, protein E

All the abaucin-children in the library targeted similar cavities at the upper part of the *A. baumannii* LolCE compared to abaucin (Figure 4 AB). Most of the LolCE amino acids targeted by **18544** and **34326** were into the E rather than into the C protein, in contrast to those predicted for abaucin docking (Table S3). More hydrogen bonds were also predicted into the E protein (3-4) compared with 1-2 into the C protein (Table S3). These amino acid preferences confirmed their higher affinity predictions towards *A. baumannii* E protein at the LolCE complex. Because of the implication of lethal mutants in the upper E region¹⁶, the similar **18544** and **34326** preferences could be implicated in experimental binding to *A. baumannii* LolCE to interact with its lipoprotein traffic activity.

Discussion

This work explores abaucin-derived chemical spaces by designing on-demand-libraries fitting their probable docking-cavities. Abaucin is a recently discovered antibiotic specifically targeting the lipoprotein transport LolCE of Gram-negative *A. baumannii*. For potential antibiotic study purposes, a new library of ~ 4000 abaucin-children molecules were computationally generated and selected by best fitting to the corresponding abaucin-LolCE docking-cavity.

The DW "Build Evolutionary library" subprogram was particular because to our knowledge, it is one of the few programs which randomly generate their own possible ligands, and select the ones targeting a unique cavity by maintaining their ligand geometries. Accurate targeting one docking-cavity favored the specific selection of the best fitting abaucin-derived children.

In particular, thousands of abaucin-children predicting higher affinities to their docking-cavity could be generated by targeting the alphafold modeled *A. baumannii* LolCE cavity. These large number of abaucin-children allowed to study an example of how undesirable docking predictions, for instance those against any commensal species, could be used to minimize antibiotic off-target effects. To retrieve a similar large number of candidates would have been impossible using more traditional screening, even if targeting the largest chemical libraries publically available (Mcule, chemSpace, Zinc, PubChem, ChEMBL, etc). Nevertheless, enormous number of alternatives still exist to be explored in the vast chemical/chemotype space^{23, 24}.

Computationally predicting chemical synthesis pathway alternatives will be the next complementary step before any *in vitro* or *in vivo* experimental studies could be undertaken. Any possible chemical synthesis may also be computationally guided by retrosynthesis predictions²⁵ (<https://rxn.res.ibm.com/>).

The described results, identified numerous new chemotypes predicting low nanomolar abaucin-children with high specificity while conserving its targeting to the predicted abaucin-docking cavity. Further work needs to include chemical synthesis for experimental validation.

Supporting information

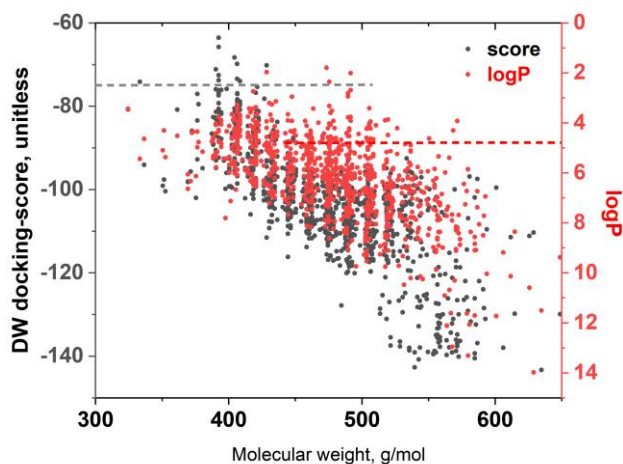


Figure S1
Resulting molecular weight and LogP profiles of abaucin-children from evolutionary docking without any other criteria than DW docking
The DW evolutionary docking of abaucin was applied only with the minimal docking-score criteria (maximal affinity), without any other criteria. Non-toxic children were represented.
Horizontal dashed red line, DW clogP of abaucin.
Horizontal dashed gray line, DW docking-score of abaucin.

Table S1
Characteristics of abaucin-children generated with different molecular weight criteria (Figure 2)

docking cavity	<MW	Raw	Fitting children	%	Nontoxic children	%
DW	-----	46067	6707	14.5	1034	15.4
ADV	<300	45667	6751	14.8	4071	60.3
ADV	<450	45879	7070	15.4	3613	51.5
ADV	<550	33387	4881	14.6	2107	43.1
DW	<390	42403	6240	14.7	3486	55.8
DW	<500	39992	6100	15.2	4260	69.8
DW	<550	41861	6178	14.7	3649	59.1

Initial parent: abaucin.sdf

Initial LoICE docking cavity: ADV or DW *A.baumannii*-abaucin cavity.pdb

Evolutionary criteria and relative weights(x): fitting to abaucin-cavity (x4); < MW (x2); logP<4 (x1).

16 children were saved from 128 children per generation, 3 runs per experiment

<MW, children maximal preferential molecular weight criteria (x4) chosen to fit during evolution

Raw, total number of randomly generated children per experiment,

Light blue vertical backgrounds, calculated percentages

Fitting, raw children fitting the cavity and their % calculated by the formula $100 \times \text{fitting children} / \text{raw}$

Nontoxic, non-toxic children and their % calculated by the formula: $100 \times \text{non-toxic children} / \text{fitting children}$.

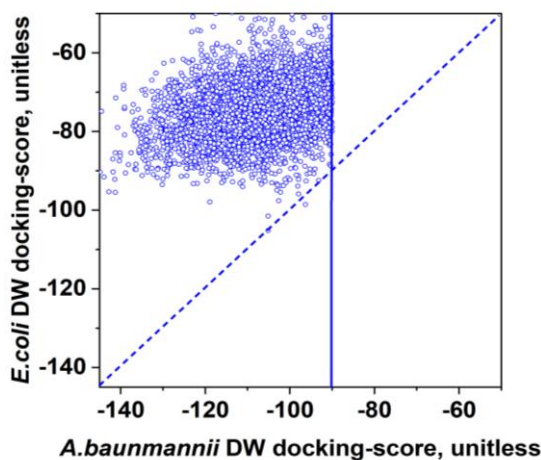


Figure S2

DW docking-scores of abaucin-children docked to *A.baumannii* and *E.coli* LoICE

The DW *A.baumannii* abaucin-children were DW docked using the *E.coli* docking cavity.

Dashed Blue line, expected data if *A.baumannii* and *E.coli* predicted similar affinities.

Vertical straight line, DW -90 docking-score threshold to select for high-affinity abaucin-children.

Table S2
Representative *A.baumannii* LoICE chemotype properties and predictions

ID	MW g/mol	logP	DW A.baum	DW E.coli	ADV,nM A.baum	LE	LLEP
abaucin	390	4.0	-71	-60	414	0.31	8.0
18544	542	0.6	-114	-71	77	0.25	2.4
34326	485	-0.5	-105	-71	65	0.28	-1.8

Each of the ID numbers were automatically assigned by the DW during evolutionary docking

Table S3
Amino acid residues of *A.baumannii* LoICE predicting contacts with representative abaucin-children

Protein	position	Aa	Aa	abaucin	18544	34326
C	88	F	Phe		H	
	92	L	Leu			
	96	I	Ile			
	292	E	Glu			
	293	L	Leu	H		
	294	F	Phe			
	296	A	Ala			
	297	V	Val			
	300	E	Glu	H		
	E	52	F	Phe	H	
53		E	Glu			
56		L	Leu		H	H
261		Y	Tyr			
262		M	Met		H	H
264		N	Asp			
265		N	Asp			H
266		I	Ile		H	H
267		Q	Gln			
***268		M	Met			
269		V	Val			
***367		Y	Tyr	H		

Aa, Amino acid residues of the *A.baumannii* LoICE docking-cavity.

Colored rectangles, amino acid residues predicted as contacts by LigPlus

H, predicted Hydrogen bonds by LigPlus.

***, lethal *E.coli* E mutants mapped to this *A.baumannii* E sequence¹⁶

Funding: This research was not externally funded

Competing interests

The author declares no competing interests

Authors' contributions

JC performed and analyzed the dockings, and drafted the manuscript.

Acknowledgements

Thanks are due to Norwid Behmd of DataWarrior (DW) for valuable contributions to fine tune the toxic filtering macros to apply to the generated children tables generated from DW Build Evolutionary Library.

References

- Liu, G., et al. Deep learning-guided discovery of an antibiotic targeting *Acinetobacter baumannii*. *Nat Chem Biol*. 2023; <https://doi.org/10.1038/s41589-023-01349-8>.
- Corseello, S.M., et al. The Drug Repurposing Hub: a next-generation drug library and information resource. *Nat Med*. 2017, 23: 405-408 <https://doi.org/10.1038/nm.4306>.
- Wu, H.J., et al. Drug-resistant *Acinetobacter baumannii*: From molecular mechanisms to potential therapeutics (Review). *Exp Ther Med*. 2023, 25: 209 <https://doi.org/10.3892/etm.2023.11908>.
- Novovic, K. and Jovicic, B. Colistin Resistance in *Acinetobacter baumannii*: Molecular Mechanisms and Epidemiology. *Antibiotics (Basel)*. 2023, 12: <https://doi.org/10.3390/antibiotics12030516>.
- Rahimzadeh, G., et al. Genotypic Patterns of Multidrug-Resistant *Acinetobacter baumannii*: A Systematic Review. *Adv Biomed Res*. 2023, 12: 56 <https://doi.org/10.4103/abr.434.22>.
- Sun, C., et al. Resistance mechanisms of tigecycline in *Acinetobacter baumannii*. *Front Cell Infect Microbiol*. 2023, 13: 1141490 <https://doi.org/10.3389/fcimb.2023.1141490>.
- Kumar, A., et al. Targeting multi-drug-resistant *Acinetobacter baumannii*: a structure-based approach to identify the promising lead candidates against glutamate racemase. *J Mol Model*. 2023, 29: 188 <https://doi.org/10.1007/s00894-023-05587-4>.
- Mittal, K.R., et al. Multidrug-Resistant *Acinetobacter baumannii*: An Emerging Aspect of New Drug Discovery. *Recent Adv Antiinfect Drug Discov*. 2023, 18: 29-41 <https://doi.org/10.2174/2772434417666220912120726>.
- Giannouli, M., et al. Molecular epidemiology of carbapenem-resistant *Acinetobacter baumannii* strains in intensive care units of multiple Mediterranean hospitals. *J Antimicrob Chemother*. 2009, 63: 828-30 <https://doi.org/10.1093/jac/dkp032>.
- Gallagher, P. and Baker, S. Developing new therapeutic approaches for treating infections caused by multi-drug resistant *Acinetobacter baumannii*: *Acinetobacter baumannii* therapeutics. *J Infect*. 2020, 81: 857-861 <https://doi.org/10.1016/j.jinf.2020.10.016>.
- Perez, F., et al. Global challenge of multidrug-resistant *Acinetobacter baumannii*. *Antimicrob Agents Chemother*. 2007, 51: 3471-84 <https://doi.org/10.1128/AAC.01464-06>.
- Usjak, D., et al. Targeting outer membrane protein A (OmpA) - inhibitory effect of 2-hydroxychalcone derivatives on *Acinetobacter baumannii* and *Candida albicans* dual-species biofilm formation. *Biofouling*. 2023: 1-11 <https://doi.org/10.1080/08927014.2023.2215693>.
- Leao, P.V.S., et al. Riparin-B as a Potential Inhibitor of AdeABC Efflux System from *Acinetobacter baumannii*. *Evid Based Complement Alternat Med*. 2023, 2023: 1780838 <https://doi.org/10.1155/2023/1780838>.
- Kumari, P., et al. Heterocyclic Diaryliodonium-Based Inhibitors of Carbapenem-Resistant *Acinetobacter baumannii*. *Microbiol Spectr*. 2023, 11: e0477322 <https://doi.org/10.1128/spectrum.04773-22>.
- Gopikrishnan, M. and George Priya Doss, C. Molecular docking and dynamic approach to screen the drug candidate against the Imipenem-resistant CarO porin in *Acinetobacter baumannii*. *Microb Pathog*. 2023, 177: 106049 <https://doi.org/10.1016/j.micpath.2023.106049>.
- Eduvirgem, J., et al. Antimicrobial and antibiofilm activities of desloratadine against multidrug-resistant *Acinetobacter baumannii*. *Future Microbiol*. 2023, 18: 15-25 <https://doi.org/10.2217/fmb-2022-0085>.
- Liu, H., et al. In vitro analysis of synergistic combination of polymyxin B with 12 other antibiotics against MDR *Acinetobacter baumannii* isolated from a Chinese tertiary hospital. *J Antibiot (Tokyo)*. 2023, 76: 20-26 <https://doi.org/10.1038/s41429-022-00573-z>.
- Tang, X., et al. Structural basis for bacterial lipoprotein relocation by the transporter LoICE. *Nat Struct Mol Biol*. 2021, 28: 347-355 <https://doi.org/10.1038/s41594-021-00573-x>.
- Coll, J.M. Evolutionary-docking targeting bacterial FtsZ. *ChemRxiv*. 2023, <https://chemrxiv.org/engage/chemrxiv/article-details/6405c36fc600523a3bc6b79>.
- Coll, J.M. New star-shaped ligands generated by evolutionary fitting the Omicron spike inner-cavity. *ChemRxiv*. 2023: <https://chemrxiv.org/engage/chemrxiv/article-details/6479b8cbe16ad5c57577cce>.
- Coll, J.M. Anticoagulant rodenticide novel candidates predicted by evolutionary docking. *ChemRxiv*. 2023: <https://chemrxiv.org/engage/chemrxiv/article-details/6479b8cbe16ad5c57577cce>.
- Mirdita, M., et al. ColabFold: making protein folding accessible to all. *Nat Methods*. 2022, 19: 679-682 <https://doi.org/10.1038/s41592-022-01488-1>.
- Polishchuk, P.G., et al. Estimation of the size of drug-like chemical space based on GDB-17 data. *J Comput Aided Mol Des*. 2013, 27: 675-9 <https://doi.org/10.1007/s10822-013-9672-4>.
- Mroz, A.M., et al. Into the Unknown: How Computation Can Help Explore Uncharted Material Space. *J Am Chem Soc*. 2022, 144: 18730-18743 <https://doi.org/10.1021/jacs.2c06833>.
- Schwaller, P., et al. Predicting retrosynthetic pathways using transformer-based models and a hyper-graph exploration strategy. *Chem Sci*. 2020, 11: 3316-3325 <https://doi.org/10.1039/c9sc05704h>.

Supplementary Material

- **toxicprediction.dwam**. A DW macro file to eliminate all toxic children from any *.sdf file, rename the resulting files and save them into the corresponding dwar and sdf files.

- **4312AbaucinChildrenLibrary.dwar**. A DW table containing 4312 abaucin-children. It was provided with threshold filters to their DW and ADV / LLEP-corrected docking-scores to *A.baumannii* and to *E.coli* LoICE, including each of their molecular weights and clogP properties.